Journal of Research in Pharmacy
Research Article
www.jrespharm.com

Formulation and characterization of puerarin loaded nanoparticles encapsulated in PDLG employing solvent evaporation method

Pallavi AHİRRAO[1]*, Kirti N DESHMUKH[2], Aakshi GUPTA[1], Sanjay M JACHAK#[2]

[1] Department of Pharmaceutical Chemistry, Chandigarh College of Pharmacy, CGC Landran, Mohali, Punjab.
[2] Department of Natural products, National Institute of Pharmaceutical Education and Research (NIPER), Sector-67, SAS Nagar (Mohali)-160062, Punjab, India.
*Corresponding Author. E-mail: pallavi.ccp@cgc.edu.in (P.A) Tel: 919876115171
#Co-corresponding Author. E-mail: sanjayjachak@niper.ac.in, sjachak11@gmail.com. (S.M.J) Tel: 9888235595

Received: 12 February 2024 / Revised: 2 May 2024 / Accepted: 4 May 2024

ABSTRACT: Puerarin (PU) nanoparticles were prepared by solvent evaporation method (using PDLG polymer), followed by lyophilization, in order to improve water solubility, systemic adsorption, and dissolution rate. PU pre-formulation parameters were studied, and optimization study of PU nanoparticles (PU-NPs) was carried out by employing Box–Behnken design (BBD), a response surface methodology. Under optimal conditions PU nanoparticles (PU-NPs) with mean particle size (MPS) 120.6± 0.03 nm and particle size distribution (PDI) 0.22 were prepared. The entrapment efficiency, drug loading and drug content in the PU-NPs were found to be, 90.21%, 14.56% and 98% respectively. The zeta potential at 25℃ was found to be -16.3 mV. PU-NPs were characterized by SEM, FTIR, XRD, TEM, stability, *in-vitro* release study and cytotoxicity. These results demonstrated that PU-NPs are non-cytotoxic and of smaller particle size than PU. Complete characterization of PU-NPs has shed light on their exceptional characteristics, thus making them a significant asset for subsequent research endeavors.

KEYWORDS: Puerarin; PDLG; Cytotoxicity; Solvent evaporation method; Puerarin nanoparticles; Novel formulation

1. INTRODUCTION

Indian Kudzu, also known as *Pueraria tuberosa* (Roxb. ex Willd) DC. (Fabaceae), is a perennial herb that is found across Asia, including India. Ayurveda and Chinese traditional medicine have recognized the potential of tuber and leaves of this plant for its nutritional and therapeutic benefits. The tuber is sweet and is frequently used to cure jaundice, bronchial asthma, menorrhagia, diseases of the skin, wounds, and skin illnesses [1,2]. Puerarin (PU) is major bioactive hydroxy-isoflavone, substituted by hydroxy group at position 7 and 4′ and a *β-D*-glucopyranosyl residue at position 8 by a C-glycosidic linkage, shown in Figure 1. *P. tuberosa* extract and its prominent pharmacologically active phytoconstituent PU, were reported to possess multiple activities such as anticancer [3,4], antiepileptic [5], antidiabetic [6], antifertility [7], anti-inflammatory [8,9], antioxidant [10], anti-stress [11], antiulcerogenic [12], cardioprotective [13,14], hypolipidemic [15], hepatoprotective [16], immunomodulatory [17], nephroprotective [18], nootropic [19], neuroprotective [20], and wound healing [21,22]. PU has been reported to possess very low oral bioavailability, and according to the biopharmaceutics classification system, belongs to BCS-class IV drug due to its poor intestinal permeability and solubility [23]. Thus, there is an urgent need to develop a novel formulation in order to enhance solubility and release of PU. There has been a lot of interest in developing oral formulations of PU with improved absorption.

In recent years several literature reports have been published describing improvement of oral bioavailability and the techniques employed include nanotechnology and related novel drug delivery system [11,24]. However, these approaches achieved not so much as drug loading characteristics along with associated data regarding particle size and drug release strategies. We therefore thought to explore

How to cite this article: Ahirrao P, Deshmukh K, Gupta A, Jachak Formulation and charecterization of puerarin loaded nanoparticles encapsuleted in PDLG employing solvent evapration method. J Res Pharm. 2025; 29(1): 295-309.

ISSN: 2630-6344
https://doi.org/10.12991/jrespharm.1643793

nanoparticles formulation that would be well-suited. Nanoparticles formulation using polymers possess unique physical and chemical properties due to their high surface area and minimum particle size. The FDA (Food and Drug Administration) has granted authorization for the PDLG polymer (co-polymer of PLGA), whose degradation kinetics modified by the copolymerization ratio of the monomers, and which is most frequently employed as a malleable and clinically proven polymer for the preparation of effective nano-carriers. They constitute highly penetrating nanocarriers with widespread pharmaceutical application due to their wide range of solubility, biocompatibility, biodegradability, and mechanical strength [25]. PDLG based nanoparticles can be formulated using various techniques like emulsification evaporation method, nanoprecipitation method, emulsion diffusion method and solvent evaporation method [26].

The solvent evaporation method was the first nanoparticle formulation method performed by using organic phase in which polymers can be dissolved, polar phase (water), and active pharmaceutical entities (API) intended to improve bioavailability [27]. By using high-speed homogenization or ultrasonication, the organic phase is emulsified in the polar phase containing surfactant, resulting in a dispersion that is allowed to evaporate by stirring at room temperature. Subsequently, the solution was freeze-dried for long-term storage [28,29].

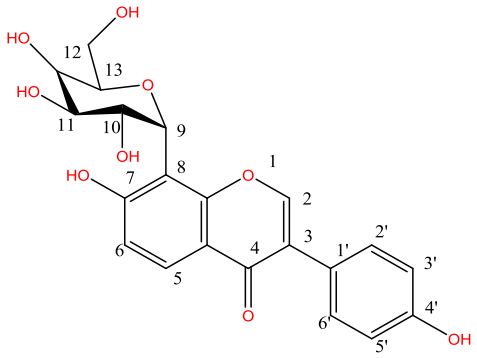

Figure 1. chemical structure of puerarin

The present research aimed to investigate whether puerarin nanoparticles (PU-NPs), may improve the release rate and provide enhanced PU physical and mechanical characteristics, in addition to enhancing the drug's bioavailability along with additional biological properties. Therefore, the Box-Behnken design (BBD) response surface methodology was employed in order to optimize the solvent evaporation procedure and achieve the ideal material ratio for PU-NP synthesis. A number of approaches were implemented to characterize the nanoparticles, including evaluating the resulting nanoparticles' cytotoxicity in RAW 264.7 (murine macrophage) cells.

2. RESULTS

2.1. Pre-formulation Studies

2.1.1. Organoleptic properties and /solubility

The PU was characterized for organoleptic properties. PU is in crystalline form with off-white color. The solubility study of PU was performed using water, acetone, methanol, chloroform, ethyl acetate, hexane and ethanol as solvent as per British Pharmacopoeia specifications. PU was sparingly soluble in water, soluble in ethanol, methanol, ethyl acetate and acetone and was insoluble in chloroform and hexane.

2.1.2. Melting point/pH Determination

The melting point of PU was determined by assessing the range of temperatures viz initial melting temperature, full melting temperature, with melting range and time required. The initial melting temperature was found 182^{0}C, full melting temperature was 185^{0}C, melting range 4 and time 27 minutes. The pH of PU was determined employing a pH meter, and was observed as 7.01.

2.1.3. Calibration curve

Calibration curve of PU was plotted using serial dilution of PU from 1mg/ml stock. Aliquots of dilutions (50, 25, 12.5, 6.25, 3.25, 1.25 µg/ml) were formed. The relationship between PU concentration and absorbance was obtained by data processing, the calibration curve showed good linearity relationship in the range of 50-1.25 µg/ml (R^2>0.99), Figure 2.

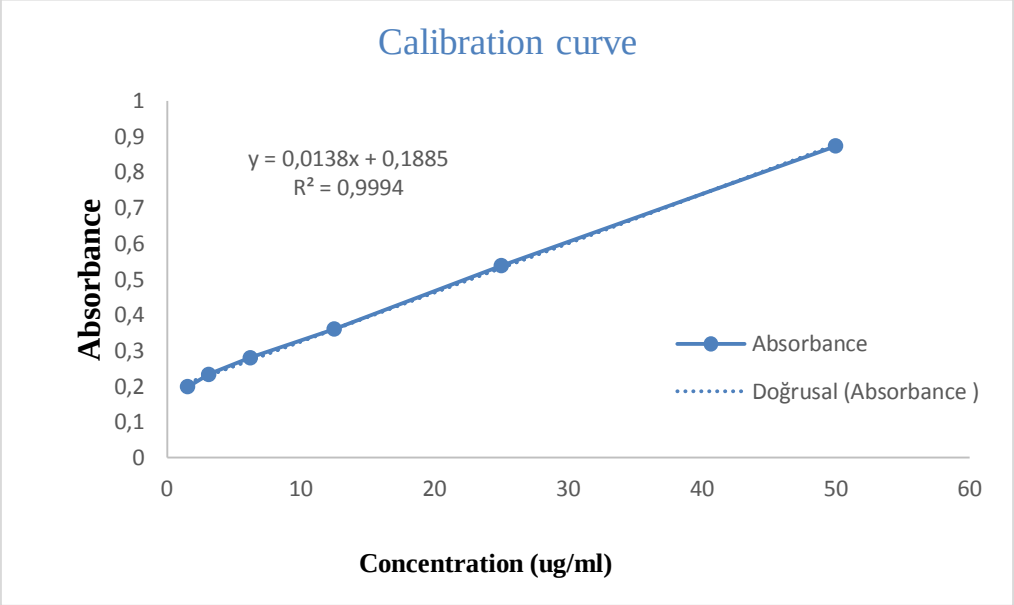

Figure 2. Calibration Curve of PU

2.1.4. Partition Coefficient (log D) and Dissociation Constant (pKa)

The UV absorbance of PU was recorded for both the phases (octanol and water) and calculated the concentration in each phase the value of log D obtained is 0.50. The p*K*a of PU was determined in six different buffer solutions using UV spectrophotometer, pKa value of the PU at different pH listed in Table 1.

Table 1. pKa values at different pH rang

pH	Absorbance	pKa=pH+log (di −d/d−dm)
6.0	0.251	6.08
6.2	0.319	6.26
6.4	0.340	6.45
6.6	0.432	6.64
6.8	0.569	6.83
7.0	0.621	7.02

2.2. Optimization of PU-NPs

Depending on the 17 confirmatory runs of PU-NPs designed by BBD, all the responses of these runs were analyzed using Design-Expert software (Version 8.0.7.1) and fitted best to the quadratic model ($p < 0.0001$) with a significant lack of fit ($p > 0.05$). A total of 17 formulations were evaluated and rank ordered according to BBD. The quadratic model's F value was 27.71, demonstrating that it constituted a significant model. Table 2 depicts how the two independent variables, polymer amount (F1) and probe sonication time (F2), positively impacted the size and entrapment efficacy of PU-NPs.

Table 2. Listed independent values and response for PU-NPs in Box–Behnken Design (BBD)

Run	F1: PDLG (mg)	F2: probe sonication (min)	R1: particle size (nm)	R2:EE (%)
1	100	3	286	82
2	100	1	282	85
3	50	1	290	49

4	50	3	286	45
5	100	3	120	90
6	100	2	120	90
7	150	1	598	72
8	150	2	625	70
9	150	3	665	75
10	100	2	120	90
11	100	1	282	85
12	100	2	120	90
13	150	2	625	70
14	50	2	270	49
15	100	2	120	90
16	50	2	270	49
17	100	3	285	82

According to the characterization results, PDLG concentration (F1) was determined to be crucial among all the parameters owing to its substantial impact on PU-NP particle size. Increasing the PDLG concentration up to 150 mg leads to an increase in particle size in the formulation. It emerged as evident from this experiment that the development of PU-NPs was only conceivable at specific PLGA concentrations in order to formation of any nanoparticles. The sonication time also affects particle size and entrapment efficiency (EE) significantly [24]. Consequently, it was determined that a particular sonication time (2 min) with an optimum PLGA concentration (100mg) favoured the formation of nanoparticles with a smaller particle size (120 nm) and the highest EE (90%) found in the present study (Table 2).

2.2.1. Optimization and validation of parameters

The significant characteristics of the model terms was indicated via the model's *p* value, which was less than 0.0001. The interaction effects of the two independent variables i.e., polymer amount (F1), and probe sonication time (F2), and on two dependent variables such as particle size (R1) and entrapment efficiency (R2) were studied by 3D response surface plots (Figure 3c and d) [30]. The effect of independent variables on response such as particle size was exhibited in the contour map provided in Figure 3 a and b.

A minimum size of PU nanoparticles and maximum entrapment efficiency were set as the criteria for the optimization of PU-NPs parameters. The optimal parameters for preparing PU nanoparticles with the smallest particle sizes and maximum entrapment efficiency were predicted as F1 polymer amount 100mg and F2 probe sonication time 2 min, as discussed earlier (Table 3). To verify whether the predicted parameters were the best parameters, nanoparticles were prepared according to the predicted parameters, and the actual response values (particle sizes and entrapment efficiency) were obtained. Relative errors were calculated for comparing the predicted values and actual values, and the relative error was below 5%, indicating a little variation in the batches [31].

Table 3. Predicted and actual values for the formulations in optimization process

Batch No	Independent Variables		Response (size, entrapment efficiency)				
			Observed		Predicted		Relative Error
	F1 (mg)	F2 (min)	R1 (nm)	R2 (%)	R2 (%)	R2 (%)	

1	100	2	119.6	89.6	120	90	0.40%
2	100	2	119.82	89.86			0.15%
3	100	2	118.308	88.731			1.41%

The most efficient formulation emerged for further studies following the results demonstrated that the displayed parameters were the most effective ones for formulating nanoparticles with minimal particle sizes and optimum entrapment efficiency.

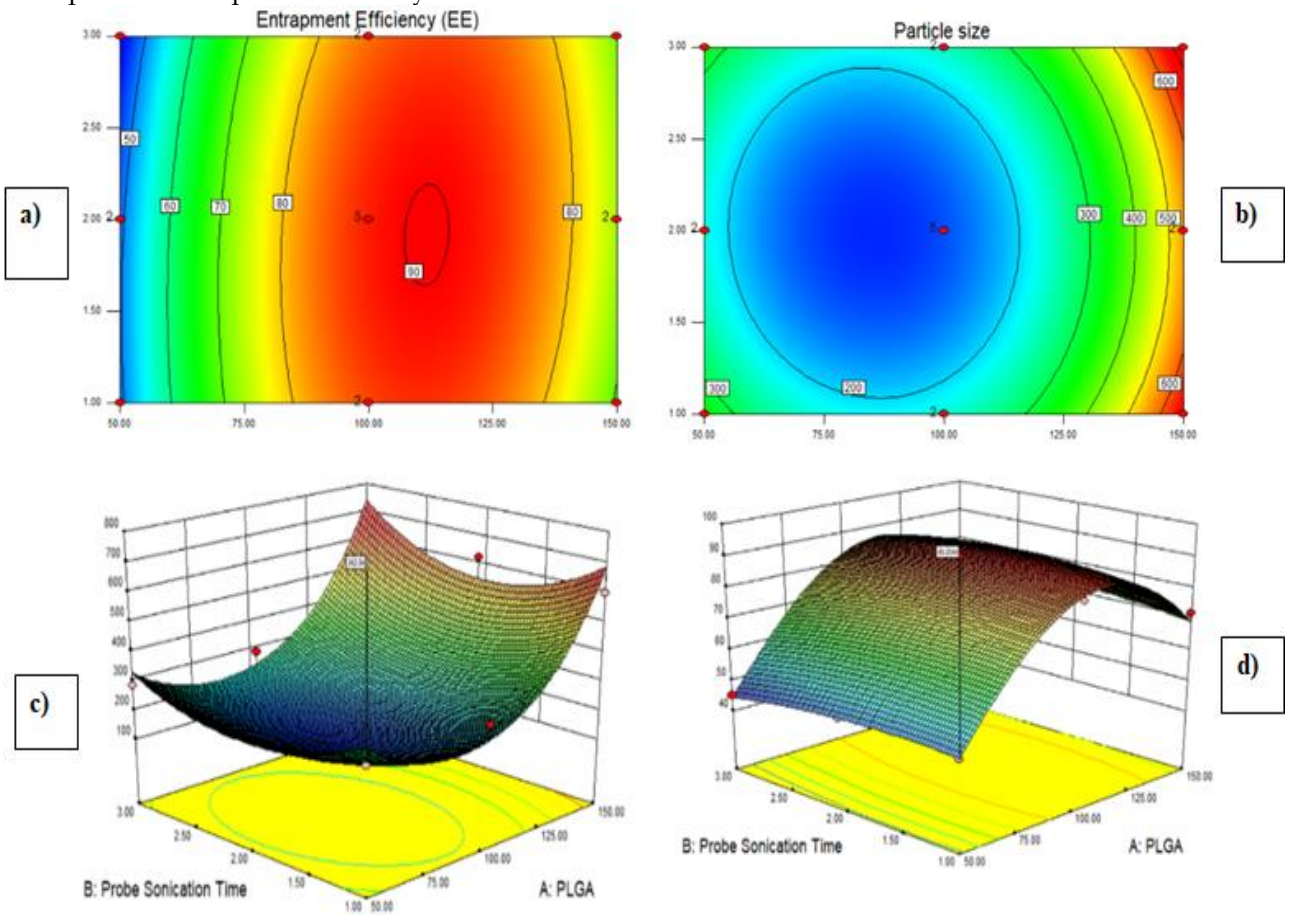

Figure 3. Two-dimensional contour map (a and b) and three-dimensional response surface plots (c and d) for the graphical optimization of PU-NPs showing interaction effect of polymer amount (F1), and probe sonication time (F2), particle size (R1) and entrapment efficiency (R2)

2.3. Characterization of PU-NPs

2.3.1. Particle size, morphology, zeta potential

The PU-NPs (Figure 4b) particle appeared as spherical shaped and smaller when measured via transmission electron microscopy (TEM) Dynamic light scattering (DLS) was used to determine the Particle Size 120.6± 0.03nm with count rate 346.7 Kcps. Perhaps, result of variations because of the measuring conditions and sample size. The TEM technique employed measurement of dry particles sphere area with less sample size, while the DLS approach employing suspended particles in suspension calculated the hydrodynamic size of particle core as well as the surrounding solvent layer as the particles moved in a Brownian motion and exceed amount of sample size. The results were displayed as an intensity-based Particle Size Distribution (Figure 4a). The developed PU-NPs exhibited poly dispersity index (PDI) of 0.22 with count rate 346.7 Kcps, and their zeta potential, estimated at 25°C employing the Delsa nano zeta-sizer,

was -16.3 mV. A high negative charge implies the establishment of a stable system of nanoparticles that will be less inclined to aggregate while stored for a prolonged period of time (Figure 4c).

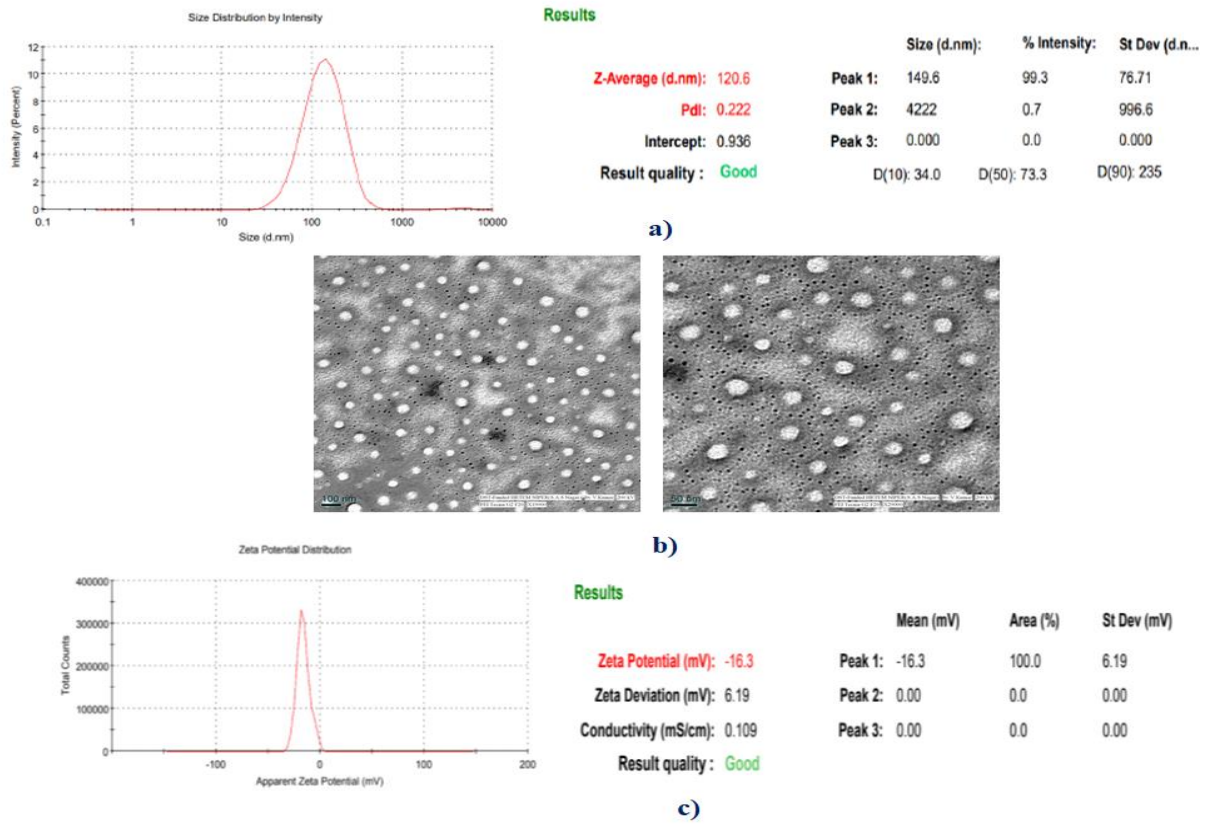

Figure 4. a) Observed Zeta Sizer Graph of PUNPs, b) SEM pictures of PU-NPs, and c) observed zeta potential of PU-NPs

2.3.2. Drug Loading (DL), Encapsulation Efficiency (EE), and Drug Content

The drug loading, encapsulation efficiency, and drug content in the PU-NPs were observed to be, 14.56%, and 90.21%, 98%, respectively.

2.3.3 XRD analysis and FTIR analysis

XRD analysis was employed to study the potential changes of the crystalline state of PU in PU-NPs. The XRD patterns for PU and PU-NPs are provided in Figure 6. While, compared the diffractograms of PU-NPs and pure PU, it was observed that almost all of the diffraction peaks disappeared demonstrating that PUE-NPs are in an amorphous form. Therefore, these results shows that nanoparticles are more stable than the PU. The FTIR analysis was carried out to evaluate the possible interaction between the drug and excipient which are used for formulation preparation, it determines possible interactions by vibration modes of the specific functional group active drug and excipient used in the formulation. The FTIR spectrum of PU, Pluronic, PDLG, and PU-NPs showed characteristics peaks (Figure 5). The FTIR spectrum of PU showed characteristic peak at 3376.89 cm^{-1}, 2918.27, cm^{-1} and 892.29 cm^{-1} stretching vibrations and the anti-symmetric stretching vibration of O-H group associated with alcohol or phenol and also, peak at 1654.07 and 1514.44 cm^{-1} were relates band Stretching of aldehyde group and C=C group of A ring and C ring of PU respectively. The bending vibration at 1446.50 cm^{-1}, and stretching vibration at 1062.80 cm^{-1} reveled CH_2 group and secondary alcohol of glucopyranose ring. When, IR of PU absorption compared to PU-NPs demonstrates certain variations, notably a slight shifting of broad peak at 1654.07 and 1514.44 cm^{-1}. However, no new characteristic peak development was seen, which may provide compelling proof that no new chemical bond has been created. All results revealed that PU does not participate in the polymerization rection and as mentioned above the reduced broad peak was because of only encapsulated PDLG possibly formed

intermolecular forces such as hydrogen bond.

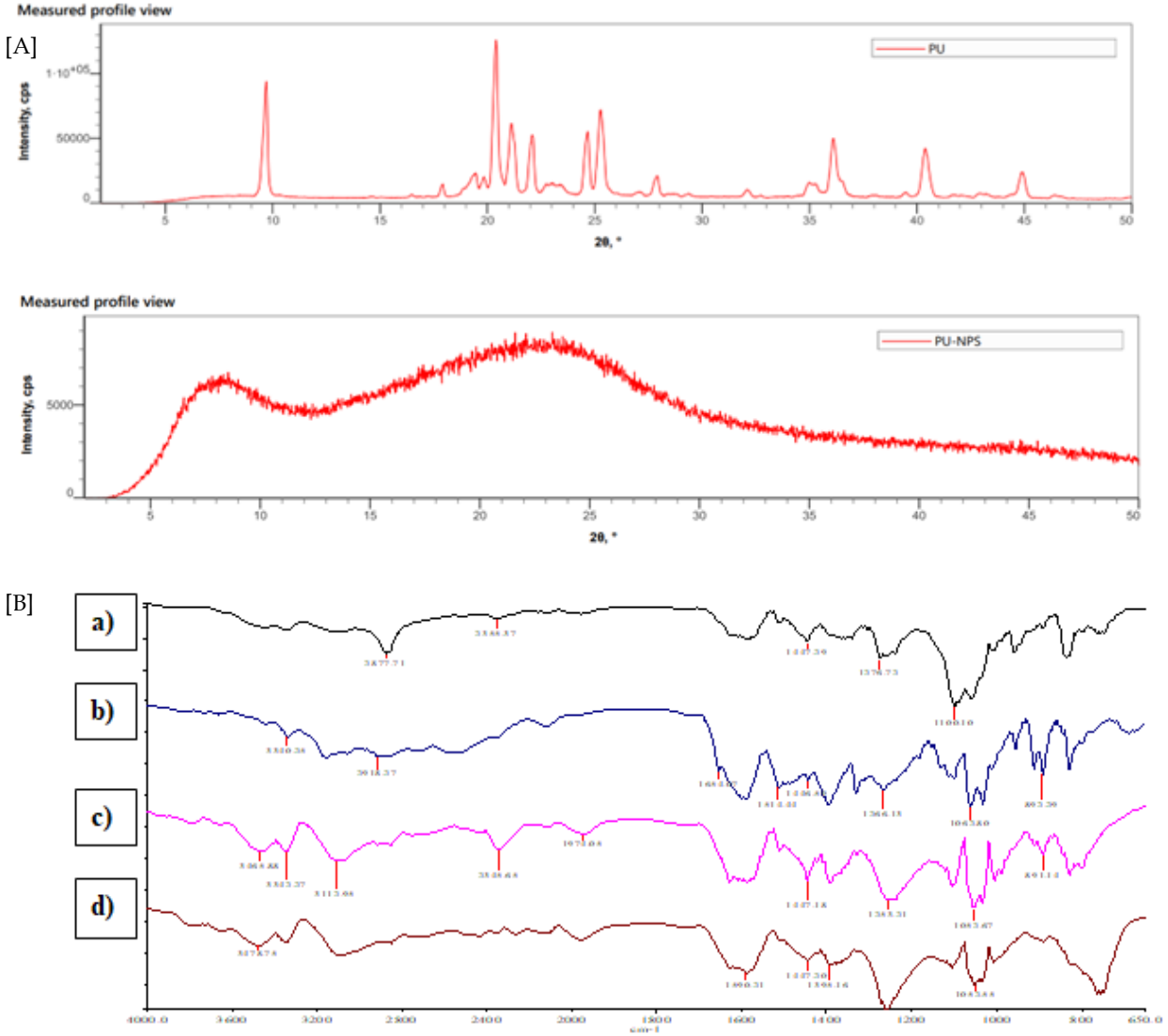

Figure 5. [A] XRD diffractograms of PU and PU-NPs, [B] FT-TR Spectra of a) Pluronic, b) PU, c) PU Nanoparticles, d) PDLG

2.3.4. In Vitro Drug Release Studies

Assessment of physical stability of PU-NPs was determined by using simulated gastric fluid (SGF; pepsin, pH 1.2), and intestinal fluid (SIF; trypsin, pH 6.8) based on United State Pharmacopeia (USP) showed PU-NPs are stable at all pH for 6 hr.

The *in-vitro* drug release of a PU nanoparticles formulation is shown in Figure 6. The release of PU from the nanoparticle's was 80.322±0.206 % within 24hrs. (Figure 6) Therefore, consequently evident that the formulation demonstrated prolonged drug release. Estimating the release mechanism and comparing release profiles are significant applications for mathematical models. The log of log % drug release vs. log time (Korsmeyer and Peppas Exponential Equation), log of log percent drug release vs. square root of time (Higuchi plot), log of log percent drug release vs. time (zero order), and log of percent drug release vs. time (first order) were plotted for the optimized formulation. The Higuchi model was found to provide the best fit to the release data (R2 = 0.9187) while considering along the determination coefficients. The results indicate that the PU released from PU-NPs over a prolonged time.

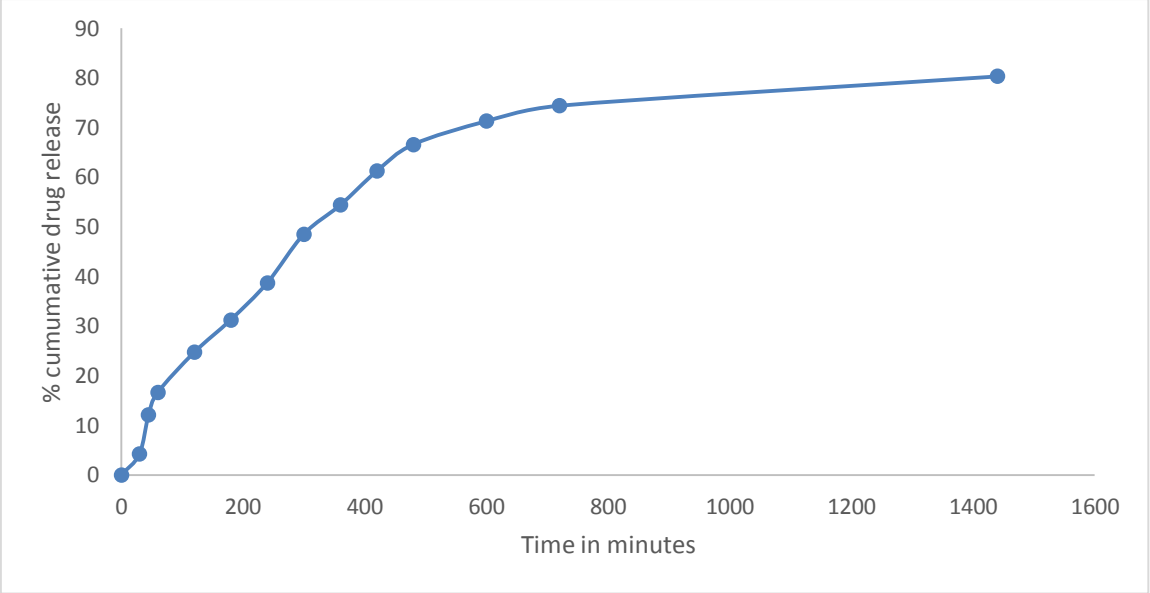

Figure 6. *In-Vitro* Drug release of PU Nanoparticles

2.3.5. Cell viability study

The cell viability of control group (non-treated) was designated 100%, indicating no cytotoxicity. Test samples PU and PU-NPs at the concentrations of 2, 5, 20 and 50 µg/mL did not affect the cell viability and showed % cell viability of 89-100% at all the concentrations with respect to the control (Figure 7). Furthermore, the incorporation of PU in PDLG in PU-NPs enhanced the viability of the PU as shown in Figure 7.

3. DISCUSSION

PU has limited absorption, poor bioavailability, and solubility. The nanotechnology has advanced significantly over the past few decades as one of the drug delivery strategies. A variety of nanotechnologies, including microemulsions, self-micro emulsifying drug delivery system (SMEDDS), dendrimers, nanoparticles, and nanocrystals, were employed to enhance PU's bioavailability. One of the previously known phospholipids complex formulations has been reported to enhance bioavailability of PU by 1.46-fold as compared to its oral suspension [32]. In prior studies on PU loaded PLGA nanoparticles showed bigger and non-uniform particle size as well as suboptimal entrapment efficiency [33-36]. By contrast 90% entrapment efficiency with higher drug content with long term stability was achieved for the PU-NPs described in present study. Additionally, our study involved a more thorough and comprehensive assessment on preparation of PU-NPs by solvent evaporation method and optimizing it by Box–Behnken design (BBD), a response surface methodology.

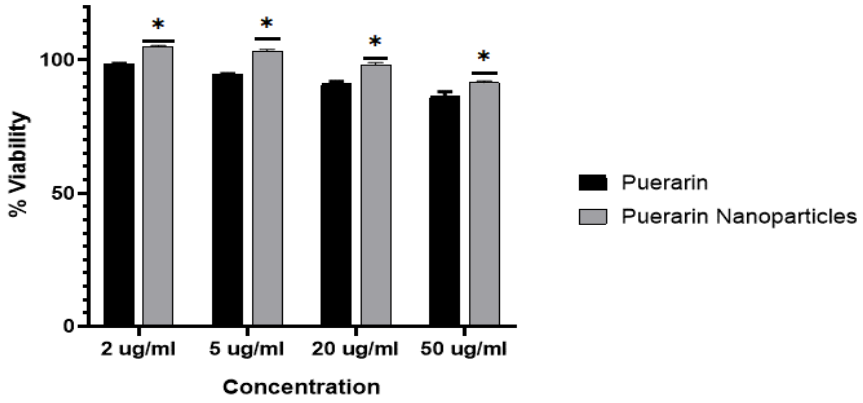

Figure 7. % vaiblity comparision of PU-NPs to PU differnat concentration *significant difference ($P < 0.05$)

Herein, for the first time we report a successful preparation of PDLG (copolymer of PLGA with high sustainable property) based PU-NPs for oral administration by utilizing solvent evaporation method with minimal particle size, count rate (346.7 Kcps), high entrapment efficiency, drug loading and drug content which is suitable for various applications in drug delivery, Nanodroplets of organic phase were formed by application of shear stresses using external energy source (probe sonicator) which is a crucial step in the solvent evaporation method. PU nanoparticles were prepared after various pre-formulation studies viz. organoleptic properties, melting point, calibration plot, pH, partition coefficient and dissociation constant.

Box–Behnken design (BBD), a response surface methodology, was implemented for optimizing PU–NPs. Two independent variables, such as polymer amount (F1), probe sonication time (F2), and the particle size (R1) and entrapment efficiency (R2) as dependent variables were selected based on the results of initial and subsequent pre-optimization research as mentioned above and shown in Figure 3. When the PDLG concentration (independent variable F1) was raised to 150 mg, a linear mode of impact emerged which increased the particle size. This might be attributed to higher viscosity, which reduces the net shear forces that may led the nanodroplet to break down. Increased probe sonication time (independent variable F2) reduced particle size because of excessive particle breakdown. Figure 2 demonstrates that when significant net shear forces were applied, the encapsulation efficiency increases. This might have occurred because less turbulent flow resulted in the effective entrapment of PU into PUNPs. The particle size distribution (PSD) of the PU-NPs has been determined to be effective, centered on their morphology, and was confirmed to be spherical shaped and small in size when assessed by employing TEM in contrast with DLS.

Zeta potential of PU-NPs was determined at 25°C (as illustrated in Figure 4a). The high negative zeta potential suggested establishment of electrically stable nanoparticles that was considerably less inclined to form agglomerate being stored for a prolonged period of time, because of repulsive forces exceed the attractive forces helps to attain physical colloidal stability. The FTIR data of PU-NPs demonstrated that PU encapsulated in PDLG primarily through potential intermolecular forces, such as hydrogen bonds and did not participate in the polymerization reaction. Potential alterations in the crystalline state of PU in PU-NPs have been explored using XRD analysis. PU-NPs are in an amorphous form, illustrated by the diffractograms for PU-NPs, whereby almost all of the diffraction peaks disappeared when compared to those with PU. These results consequently demonstrated that PU-NPs exhibited greater resilience than PU. Moreover, by analyzing the results of the MTT assay for the cell viability, we verified that PU-NPs, at concentrations of 2, 5, 20, and 50 µg/mL, were not cytotoxic compared to PU. In the present study, robust characterization data and the exceptional characteristics exhibited by PU-NPs position them as a valuable formulation for the wide range of applications. Further, *in-vivo* studies are warranted for determining anti-inflammatory activity and bioavailability studies of PU-NPs.

4. CONCLUSION

In this study, a simple technology using solvent evaporation method for the formulation of PU nanoparticles (PU-NPs) was conducted and evaluated, which produced PU-NPs for enhanced release rate. Freeze-dried PU-NPs could provide potential spherical shape, relatively small size, low PDI, and high negative zeta potential. Additionally, FTIR study demonstrated that they do not show any interaction with polymer. XRD study revealed that after converting PU in PU-NPs showed more stable amorphous form. Collectively, all characterization data of PU-NPs compared to PU indicate the enhanced potential for these nanoparticles to remain stable and dispersed, making them suitable for various applications in drug delivery, nanomedicine, or other fields where controlled particle size and stability are crucial.

5. MATERIAL AND METHODS

5.1. Materials

PU (purity, 97.2%) provided by the Department of Natural Products, NIPER, Mohali. Polymer PDLG 5002A (50/50 DL-lactic/Glycolide copolymer) was a gift sample from Corbion, Purac Biochem BV Netherlands. Surfactant Pluronic F_{127} was obtained from Sigma-Aldrich Chemicals Pvt. Ltd. (U.S.). Ethyl acetate was obtained from Labogens, India. Methanol, ethanol, potassium dihydrogen Phosphate were procured from Thomas Baker (Chemicals) Pvt. Ltd. Chloroform was obtained from Qualikems Chem Pvt. Ltd. Hydrochloric acid was obtained from SD Fine-chem. Ltd, Mumbai. Acetone was obtained from Advent Chembio Pvt. Ltd. *n*-Octanol was obtained from Research Lab Fine Chem Industries. Sodium hydroxide was obtained from Fisher Scientific India Pvt. Ltd. All other reagents used in study were of analytical reagent grade.

5.2. Preparation of PU-NPs

PU nanoparticles were prepared using solvent diffusion evaporation method, followed by lyophilization [37]. A pictorial representation of a process to prepare PUENs is provided in Figure 8. The organic phase was prepared by dissolving 4 mg of PU and 100 mg of PDLG polymer, in 1.8 ml of ethyl acetate: ethanol (30% v/v) which is equivalent to 5.5% weight, to produce a translucent, relatively viscous solution. The aqueous phase (surfactant solution) was prepared mixing Pluronic F127, (0.2gm) equivalent to 2% in 10 ml water. The organic phase was then added dropwise in aqueous phase with continuous stirring using the magnetic stirrer for 20 min at 1000 rpm resulting formation of O/W pre-emulsion. O/W pre-emulsion was curtailed by probe sonication at amplitude 30 for 2 min with pulse sequence of 30 seconds.

Then O/W primary emulsion was added to 10 mL of water with enduring stirring to diffuse and evaporation of organic phase afforded nanoprecipitation and formation of colloidal suspension. The suspended nanoparticles were subjected to centrifugation at 10,000 rpm, -5°C temperature for 20 minutes, and washed repeatedly with water to remove excess surfactant and lyophilized to obtain dried powder.

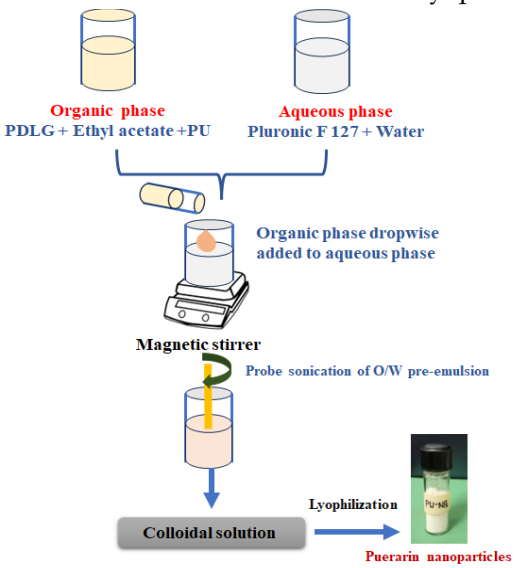

Figure 8. The experimental process for PU nanoparticles formulation by solvent diffusion evaporation method

5.3. Pre-formulation studies of PU

5.3.1. Melting Point

The melting points of PU was recorded using by melting point apparatus (Remi Equipment, Mumbai). 3 mg of PU was placed in a thin-walled capillary 10-15 mm long, and about 1 mm diameter, closed at one end [38].

5.3.2. Solubility Studies

The solubility study of PU was carried out in different solvents viz water, acetone, methanol, chloroform, ethyl acetate and ethanol as per British Pharmacopoeia [39].

5.3.3. pH determination

pH of PU was determined by utilizing a digital pH meter, test sample was prepared by shaking PU in water for 5 min followed by making 1% w/v dispersion [40].

5.3.4. Partition Coefficient (log D)

PU 1 mg was added in 5 ml of *n*-octanol: water (pre saturated) and both phases were shaken by mechanical shaker for 24 hours. After 24 hours. Both the phases were separated. UV absorbance was recorded for both the phases and the concentration of PU was calculated in each phase [41].

5.3.5. Dissociation Constant (pKa)

The pKa of PU was determined using UV spectrophotometric method as described Albert and

Serjeant (1962). Six different buffer solutions having pH in the range of 6.0 to 7.0 were prepared using stock solution of 0.2 M potassium dihydrogen phosphate and 0.2 M sodium hydroxide to give final buffer molarity of 0.2 M. Six test tubes were labelled according to the buffer capacity and added 5ml buffer solution in the respective test tube. Stock solution (2mg/ml) of PU was prepared in methanol and 50 µl of it was added in each test tube to give final PU concentration of 20µg/ml. These solutions were thoroughly mixed and placed the test tube in thermostat bath at 25°C for 10-15 minute. The absorbance of neutral and ionic species of PU determined in similar manner employing 0.01 N HCl and 0.01 M NaOH respectively at 393 nm [42].

5.4. Optimization of PU-NPs

Optimization of polymer concentration and sonication time: In order to establish the maximal drug loading capacity of the nanoparticles while minimizing particle size, the PU-NPs were further modified with respect to the PDLG polymer using different polymer drug ratio mentioned in table 2. The sonication time duration ranged from 1 min to 4 min and investigated their effect on particle size, PDI, zeta potential and entrapment efficiency of PU-NPs [43].

5.4.1. Experimental Design for optimization of PU-NPs

A response surface methodology termed Box–Behnken design (BBD) was implemented to optimize PU-NPs [24]. Based on the insights from initial and subsequent pre-optimization studies, two independent variables, such as polymer amount (F1) and probe sonication time (F2), and as a dependent variable, the particle size (R1) and entrapment efficiency (R2) were chosen. The Design-Expert program (Version 8.0.7.1) was used to design 17 batches for the experimental trials. Maximum entrapment efficiency and lowest particle size were primary selection criteria for the most suitable nano-formulation.

5.5. Characterization of PUNPs

5.5.1. Particle size, PDI and Zeta potential

PDI, zeta potential and Average particle size and were measured using dynamic light scattering using Malvern zeta sizer (ZS90). The sample of PU-NPs was analyzed directly, experimental preparation was performed on three separate occasions, and the data was obtained simply averaging the three measurements.

5.5.2. TEM Analysis

The surface morphology of PU-NPs was ascertained by TEM. The required amount of PU-NPs suspension was filled by using TEM grid. Finally, sample was analyzed by using TEM (FEI Tecnai G2F20, Netherlands) [44].

5.5.3. Fourier transform infrared spectrometer (FTIR)

FTIR analysis was performed to provide further information related to drug polymer interaction using an FTIR spectrometer (Perkin Elmer instrument) calibrated by polystyrene film. FTIR spectra of PU, PDLG, PLU and PU-NPs, were recorded using required samples amount and mixed with potassium bromide, disk were compressed for scanning. IR spectra of samples were recorded within the frequency range 4000 to 650 cm−1 [45].

5.5.4. Powder XRD analysis

Utilizing a copper radiation source as the anode material, the Rigaku Ultima IV entirely automated high resolution X-ray diffractometer (Tokyo, Japan) was employed to determine the X-ray diffraction patterns for PU and PU-NPs. Over a range of 5 to 50°, the diffraction was recorded in a step scan model with a voltage of 40 kV having a current of 40 mA with a step size of 0.02θ [46-47].

5.5.5. Drug content determination

The content of drug encapsulated in the prepared PU nanoparticles was determined by using UV spectrophotometric method. In Brief, 100µl of PU nanoparticles solution (1mg/ml, dissolved in distilled water) was mixed in methanol to determine its absorbance using UV spectrophotometric method. Standard plot of drug is prepared for determination of concentration and drug content [48].

5.5.6. Drug Loading (DL)and Encapsulation Efficiency (EE)

Employing the centrifugation ultrafiltration method, the drug loading and encapsulation efficiency of PU nanoparticles were determined [31]. Through centrifugal filter tubes, the free PUE was separated from the PU-NPs. In simple terms, a centrifugal filter tube was filled with 2 mL of the PU-NPs suspension, and the tube was centrifuged for twenty minutes at room temperature at 4000 rpm. By employing a UV spectrophotometric approach, the initial concentration of PU in the suspension and the amount of free measured. The following formula was implemented for estimating the drug loading and encapsulation effectiveness of the PU-NPs:

$$EE\% = [\, W_{total\ drug} - W_{free\ drug} / W_{total\ drug} \,] \times 100\%, \qquad \text{(Equation 1)}$$

$$DL\% = [W_{total\ drug} - W_{free\ drug} / W_{polymer} \,] \times 100\%, \qquad \text{(Equation 2)}$$

Where, "$W_{free\ drug}$" is the amount of PU unloaded in PU-NPs, "$W_{total\ drug}$" is the initial total amount of PU in the suspension, and "$W_{polymer}$" is the weight of PDLG.

5.8. Drug Release Studies

5.8.1. Assessment of stability PU-NPs and Release Studies

Physical stability of nanoparticles was evaluated using three different simulated fluids as per United States Pharmacopeia (USP) stability guidelines, simulated gastric fluid (SGF; pepsin, pH 1.2), simulated intestinal fluid (SIF; trypsin, pH 6.8) and phosphate buffered saline (PBS; pH 7.4) were taken and 10 ml of each combined with 1 ml of PU-NPs at 37°C with shaking. The mixture was then evaluated using dynamic light scattering (DLS) at various time points viz 0, 1, 2, 4, and 6 hours.

Using phosphate buffer solutions (PBS, pH 7.4) with a 12–14 kDa molecular cutoff bag, dialysis was performed to investigate the in vitro release of PU from the PU-NPs. Dialysis bags were filled with 5 mL of PU-NPs solution. Subsequently, the bags were placed inside flasks containing 150 mL of PBS as the dissolution media, these was shaken at 100 rpm in a 37°C water bath. At regular intervals, one milliliter of the dissolving medium was withdrawn, and the same volume was substituted with fresh media. The UV spectrophotometric approach was employed to measure the amounts of PU in the dissolving medium [26].

5.8.2. Calibration Plot

PU (1 mg) was dissolved in 1ml methanol in an Eppendorf tube, and diluted to give 100 µg/ml standard sample was prepared. Aliquots of standard solutions (50, 25, 12.5, 6.25, 3.25, 1.25 ug/ml) were prepared. The samples were measured by UV spectrophotometric method at wavelength 250nm.

5.9 Cell viability studies:

Cell viability was assessed using MTT assay. Briefly, RAW 264.7 murine macrophages cells were seeded into a 96-well plate at a density of 2×10^5 in DMEM medium per well and incubated overnight. During treatment, the medium was replaced and PUNPs solution of different concentrations (12.5–200 µg/mL) or LPS (1.0 mg/mL) dissolved in DMEM, and it was incubated for another 24 h. Following the incubation and treatment of 24 hours, 10 µL of a 5 mg/mL MTT solution was added to each well, and the resultant mixture was incubated for four additional hours at 37° C. After four hours, the formazan crystal had remained at the bottom of the plate after the supernatant was discarded. To dissolve the undissolved formazan salt, 100 µl dimethyl sulfoxide was then added. After around 20 minutes, the plate was incubated. A microplate reader was used to quantify the formazan formed at 570 nm [49-50].

5.10 Statistical analysis

The statistical analysis of the pharmacokinetic data was carried out using a student t-test with $P < 0.05$ as the minimal level of significance, and the anti-inflammatory activity date was determined as the mean ± standard error of the mean (SEM). Statistical differences between the treatment and control groups were evaluated by a student t-test with $P < 0.05$ as the minimal level of significance. All statistical analysis was carried out using the Graph Pad Prism software.

Acknowledgements: The National Institute of Pharmaceutical Education and Research (NIPER) and the Chandigarh Group of Colleges (CGC) Landran, Mohali, are acknowledged by the authors for helping with the experimental work which is provided here. The authors would like to acknowledge their gratitude to Corbion for providing a gift sample of the polymer.

Author contributions: Concept – P.A and S.M.J.; Design – P.A.; Supervision – P.A and S.M.J, Resources – S.M.J.; Materials – S.M.J; Data Collection and/or Processing – K.N.D and A.G.; Analysis and/or Interpretation – K.N.D and A.G.; Literature Search – K.N.D and A.G.; Writing – P.A and S.M.J.; Critical Reviews – P.A and S.M.J.
Conflict of interest statement: The authors report no conflict of interest to declare.

REFERENCES

[1] Ayurvedic Pharmacopoeia of India, Department of Health, Ministry of Health and Family Planning, Government of India,New Delhi, India, 1999,Part 1 and 2, pp. 1–190.
[2] Cao S, Li X, Yin H, Wang J, Liu J. Dietary puerarin supplementation improves immune response and antioxidant capacity of sows. Antioxidants. 2024; 3: 290. https://doi.org/10.3390/antiox13030290
[3] Singh H, Kriplani P, Kamboj S, Guarve K. Puerarin: An anticancer and anti-inflammatory agent. Recent Pat Anticancer Drug Discov. 2024;19: 18-36. https://doi.org/10.2174/1574892818666230111152024
[4] Adedapo A, Fagbohun A, Dawurung C, Oyagbemi A, Omobowale O, Yakubu A. The aqueous tuber extract of *Pueraria tuberosa* (Willd.) DC caused cytotoxic effect on HT 29 cell lines with down regulation of nuclear factor-kappa B (NF-κB). J Complement Integr Med. 2017; 16(4): 20160119. https://doi.org/10.1515/jcim-2016-0119
[5] Basavaraj P, Shivakumar B, Shivakumar H. Evaluation of anticonvulsant activity of alcoholic extract of tubers of *Pueraria Tuberosa* (Roxb). Adv Pharmacol Toxicol. 2011; 12(1): 1-9.
[6] Oza M, Kulkarni A. Formononetin treatment in type 2 diabetic rats reduces insulin resistance and hyperglycemia. Front Pharmacol. 2018; 9: 739. https://doi.org/10.3389/fphar.2018.00739
[7] Gupta R, Sharma R, Sharma A, Choudhary R, Bhatnager A, Joshi Y. Antifertility effects of *Pueraria tuberosa* root extract in male rats. Pharmaceut Biol. 2005; 42 (8): 603-609. https://doi.org/10.1080/13880200490902491
[8] Pandey N, Yadav D, Pandey V, Tripathi B. Anti-inflammatory effect of *Pueraria tuberosa* extracts through improvement in activity of red blood cell anti-oxidant enzymes. AYU. 2013; 34 (3): 297-301. https://doi.org/10.4103/0974-8520.123131
[9] Ye Z, Wu H, Chen X, Xie R, Zhang D, Sun H, Wang F, Li Z, Xia Q, Chen L, Chen T. Puerarin inhibits inflammation and oxidative stress in female BALB/c mouse models of Graves' disease. Transl Pediatr. 2024; 16 (1): 38. https://doi.org/10.21037%2Ftp-23-370
[10] Shukla R, Banerjee S, Tripathi B. Antioxidant and antiapoptotic effect of aqueous extract of *Pueraria tuberosa* (Roxb. Ex Willd.) DC. On streptozotocin-induced diabetic nephropathy in rats. BMC Complement Altern Med. 2018; 18 (1): 156. https://doi.org/10.1186/s12906-018-2221-x
[11] Verma S, Jain V, Singh D. Effect of *Pueraria tuberosa* DC.(Indian Kudzu) on blood pressure, fibrinolysis and oxidative stress in patients with stage 1 hypertension. Pak J Biol Sci. 2012; 15 (15): 742-747. https://doi.org/10.3923/pjbs.2012.742.747
[12] Sumalatha G, Awen B, Chandu B, Mukkanti K. Anti ulcerogenic & ulcer healing studies of aqueous extract of *Pueraria tuberosa* leaves on rats. Int J Pharm Bio Sci. 2010; 1 (4): 657-661.
[13] Patel V, Mistry M, Shinde K, Syed R, Singh V, Shin S. Therapeutic potential of quercetin as a cardiovascular agent. Eur J Med Chem. 2018; 155: 889-904. https://doi.org/10.1016/j.ejmech.2018.06.053
[14] Sun XY, Chen JP, Shang JJ, Liu HX, Li X, Lou Y, Zhou HW. Traditional Chinese medicine injections with activating blood circulation, equivalent effect of anticoagulation or antiplatelet, for acute myocardial infarction: A systematic review and meta-analysis of randomized clinical trials. Complementary Ther Med. 2024; 13: 103039. https://doi.org/10.1097%2FMD.0000000000029089
[15] Tanwar Y, Goyal S, Ramawat K. Hypolipidemic effects of tubers of Indian kudzu (*Pueraria tuberosa*). J Herbal Med Toxicol 2008; 2 (1): 21-25.
[16] Xia D, Zhang P, Yan F, Wei-Fu Y, and Meng-Ting. Hepatoprotective activity of PU against carbon tetrachloride-induced injuries in rats: A randomized controlled trial. Food Chem Toxicol. 2013; 59: 90-95. https://doi.org/10.1016/j.fct.2013.05.055
[17] Patel J, Doshi N, Bhalerao A, Bonagiri R. Immunomodulatory activity of ethanolic extract of *Pueraria tuberosa* DC. Int J Sci Eng Res. 2016; 7 (11): 708-713.
[18] Shukla R, Banerjee S, Tripathi B. *Pueraria tuberosa* extract inhibits iNOS and IL-6 through suppression of PKC-α and NF-kB pathway in diabetes-induced nephropathy. J Pharm Pharmacol. 2018; 70 (8): 1102-1112. http://dx.doi.org/10.1111/jphp.12931
[19] Rao V, Pujar B, Nimbal S, ShantakumarmS, Satyanarayana S. Nootropic activity of tuber extract of *Pueraria tuberosa* (Roxb). Indian J Exp Bio. 2008; 46(8): 591-598.
[20] Xing G, Dong M, Li X, Zou Y, Fan L, Wang X, Cai D, Li C, Zhou L, Liu J, Niu Y. Neuroprotective effects of puerarin against beta-amyloid-induced neurotoxicity in PC12 cells via a PI3K-dependent signaling pathway. Brain Res Bull. 2011;85(3-4):212-218. https://doi.org/10.1016/j.brainresbull.2011.03.024
[21] Kambhoja S, Murthy K. Wound healing and anti-inflammatory activity of *Pueraria tuberosa* (Roxb Ex wild) DC. Biomed. 2007; 2 (2): 229-232.

[22] Maji K, Pandit S, Banerji P, Banerjee D. *Pueraria tuberosa*: A review on its phytochemical and therapeutic potential. Nat Prod Res. 2014; 28 (23): 2111-2127. https://doi.org/10.1080/14786419.2014.928291
[23] Quan D, Xu G, Wu X. Studies on preparation and absolute bioavailability of a self-emulsifying system containing PU. Chem Pharm Bull. 2007; 55 (5): 800-803. https://doi.org/10.1248/cpb.55.800
[24] Li H, Dong L, Liu Y, Wang G, Wang G, Qiao Y. Biopharmaceutics classification of PU and comparison of perfusion approaches in rats. Int J Pharm. 2014; 466 (1-2): 133-138. https://doi.org/10.1016/j.ijpharm.2014.03.014
[25] Wang Y, Ma Y, Du Y, Liu Z, Zhang D, Zhang Q. Formulation and pharmacokinetics evaluation of PU nanocrystals for intravenous delivery. J Nanosci Nanotechnol. 2012; 12 (8): 6176-6184. https://doi.org/10.1166/jnn.2012.6436
[26] Tu L, Yi Y, Wu W, Hu F, Hu K, Feng J. Effects of particle size on the pharmacokinetics of PU nanocrystals and microcrystals after oral administration to rat. Int J Pharm. 2013; 458 (1): 135-140. https://doi.org/10.1016/j.ijpharm.2013.10.001
[27] Zielińska A, Carreiró F, Oliveira M, Neves A, Pires B, Venkatesh N, Durazzo A, Lucarini M, Eder P, Silva M, Santini A, Souto B. Polymeric nanoparticles: Production, characterization, toxicology and ecotoxicology. Molecules. 2020; 25(16): 3731. https://doi.org/10.3390/molecules25163731
[28] Bohrey S, Chourasiya V, Pandey A. Polymeric nanoparticles containing diazepam: Preparation, optimization, characterization, in-vitro drug release and release kinetic study. Nano Converg. 2016; 3: 1–7. https://doi.org/10.1186/s40580-016-0061-2
[29] Liu X, Huang R, Wan J. Puerarin: A potential natural neuroprotective agent for neurological disorders. Biomed. 2023; 1 (162): 114581. https://doi.org/10.1016/j.biopha.2023.114581
[30] Agrawal V, Patel R, Patel M. Design, characterization, and evaluation of efinaconazole loaded poly (D, L-lactide-co-glycolide) nano-capsules for targeted treatment of onychomycosis. J Drug Deliv Sci Technol. 2023; 80: 104157. https://doi.org/10.1016/j.jddst.2023.104157
[31] Rampado R, and Peer D. Design of experiments in the optimization of nanoparticle-based drug delivery systems. J Control Release. 2023; 358: 398-419. https://doi.org/10.1016/j.jconrel.2023.05.001
[32] Rashid A, Muneer S, Wang T, Alhamhoom Y, Rintoul L, Izake L, Islam N. PU dry powder inhaler formulations for pulmonary delivery: Development and characterization. Plos One 2021; 16 (4): 0249683. https://doi.org/10.1371/journal.pone.0249683
[33] Tao Q, Meng Q, Li H, Yu H, Liu F, Du D, Peng S. HP-β-CD-PLGA nanoparticles improve the penetration and bioavailability of puerarin and enhance the therapeutic effects on brain ischemia–reperfusion injury in rats. Naunyn-Schmiedeberg's Arch Pharmacol. 2013; 386: 61-70. https://doi.org/10.1007/s00210-012-0804-5
[34] Li L, Li Y, Miao C, Liu R. improved therapeutic effect of puerarin-encapsulated PEG-PLGA nanoparticle on an in vitro cerebral infarction model. Adv Polym Technol. 2020; 1-7. https://doi.org/10.1155/2020/7145738
[35] Chen T, Liu W, Xiong S, Li D, Fang S, Wu Z, Chen X. Nanoparticles mediating the sustained puerarin release facilitate improved brain delivery to treat Parkinson's disease. ACS Appl Mater Interfaces. 2019; 11(48): 45276-45289. https://doi.org/10.1021/acsami.9b16047
[36] Zhang Y, Li Y, Zhao X, Zu Y, Wang W, Wu W, Li Z. Preparation, characterization and bioavailability of oral puerarin nanoparticles by emulsion solvent evaporation method. RSC Adv. 2016; 6(74): 69889-69901. http://dx.doi.org/10.1039/C6RA08413C
[37] Bairwa K, Jachak S. Anti-inflammatory potential of a lipid-based formulation of a rotenoid-rich fraction prepared from *Boerhavia diffusa*. Pharm Bio. 2015; 53 (8): 1231-1238. https://doi.org/10.3109/13880209.2014.971382
[38] Peres C, Matos I, Conniot J, Sainz V, Zupančič E, Silva M, Graca L, Gaspar S, Preat V, Florindo F. Poly (lactic acid)-based particulate systems are promising tools for immune modulation. Acta Biomater. 2017; 48: 41-57. https://doi.org/10.1016/j.actbio.2016.11.012
[39] Bharate S, Kumar V, Vishwakarma A. Determining Partition Coefficient (Log P), Distribution Coefficient (Log D) and Ionization Constant (pKa) in Early Drug Discovery. Comb Chem High T Scr. 2016; 19(6): 461–469. https://doi.org/10.2174/1386207319666160502123917
[40] Singh S, Sharda N, Mahajan L. Spectrophotometric determination of pKa of nimesulide. Int J Pharm. 1999; 176 (2): 261-264. https://doi.org/10.1016/S0378-5173(98)00304-4
[41] Xu N, He C. Separation and purification of PU with solvent extraction. Sep Purif Technol. 2007; 56 (3): 397-400. https://doi.org/10.1016/j.seppur.2007.06.003
[42] Han E, Priefer R. A systematic review of various pK_a determination techniques. Int J Pharm. 2023; 635: 122783. https://doi.org/10.1016/j.ijpharm.2023.122783
[43] Kalam A, Khan A, Khan S, Almalik A, Alshamsan A. Optimizing indomethacin-loaded chitosan nanoparticle size, encapsulation, and release using Box–Behnken experimental design. Int J Bio Macromol. 2016; 87: 329-340. https://doi.org/10.1016/j.ijbiomac.2016.02.033
[44] Zhao L, Liu A, Sun M, Gu J, Wang H, Wang S, Zhang J, Guo C, Duan R, Zhai N. Enhancement of oral bioavailability of PU by polybutylcyanoacrylate nanoparticles. J Nanomater. 2011; 2011: 126562. https://doi.org/10.1155/2011/126562
[45] Zhang F, Liu G, Shen W, and Gurunathan S. Silver nanoparticles: Synthesis, characterization, properties, applications, and therapeutic approaches. Int J Mol Sci. 2016; 17(9): 1534. https://doi.org/10.3390/ijms17091534.

[46] Sapsford E, Tyner M, Dair J, Deschamps R, Medintz L. Analyzing nanomaterial bioconjugates: A review of current and emerging purification and characterization techniques. Anal Chem. 2011; 83 (12): 4453-4488. https://doi.org/10.1021/ac200853a

[47] Qiang S, Gu L, Kuang Y, Zhao M, You Y, Han Q. Changes in the content of PU-PLGA nanoparticles in mice under the influence of alcohol and analysis of their antialcoholism. J Appl Biomater Funct Mater. 2023; 21: 22808000221148100. https://doi.org/10.1177/22808000221148100

[48] Weng J, Tong Y, Chow F. In vitro release study of the polymeric drug nanoparticles: development and validation of a novel method. Pharmaceutics. 2020; 12(8): 732. https://doi.org/10.3390/pharmaceutics12080732

[49] Facchin BM, Dos Reis GO, Vieira GN, Mohr ETB, da Rosa JS, Kretzer IF, Demarchi IG, Dalmarco EM. Inflammatory biomarkers on an LPS-induced RAW 264.7 cell model: A systematic review and meta-analysis. Inflamm Res. 2022;71(7-8):741-758. https://doi.org/10.1007/s00011-022-01584-0

[50] Guo Z, Xu Y, Xu L, Wang S, Zhang M. In vivo and in vitro immunomodulatory and anti-inflammatory effects of total flavonoids of *Astragalus*. Afr J Tradit Complement Altern Med. 2016; 13(4): 60–73. https://doi.org/10.21010/ajtcam.v13i4.10